Extracting Phenomenology from DSEs: The $^3P_0$ Model and (Hybrid) Meson Decays

A. Salas-Bernárdez, F. Llanes-Estrada and R. Alkofer; ECT* Workshop, Trento.

29th May 2025

ECT* Workshop: The complex structure of strong interactions in Euclidean and Minkowski space

Trento, Italy

Non-perturbative calculations for hadron phenomenology

Extensive work from many different groups to compute hadron properties from non-perturbative analytical methods:

Z. N. Xu, Z. Q. Yao, D. Binosi, M. Ding, C. D. Roberts and J. Rodríguez-Quintero, Eur. Phys. J. C **85** (2025)
G. Eichmann, A. Gómez, J. Horak, J. M. Pawlowski, J. Wessely and N. Wink, Phys. Rev. D **109** (2024) no.9, 096024
M. Q. Huber, C. S. Fischer and H. Sanchis-Alepuz, Nuovo Cim. C **47** (2024) no.4, 184
G. Eichmann, E. Ferreira and A. Stadler, Phys. Rev. D **105** (2022) no.3, 034009

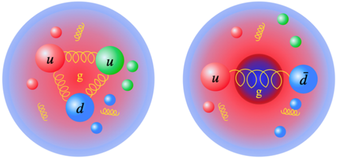

Lattice efforts to compute QCD's Green's functions:

M. Colaço, O. Oliveira and P. J. Silva, Phys. Rev. D **109** (2024) no.7, 074502
O. Oliveira, A. Kızılersu, P. J. Silva, J. I. Skullerud, A. Sternbeck and A. G. Williams, Acta Phys. Polon. Supp. **9** (2016), 363-368
O. Oliveira, W. de Paula, T. Frederico and J. P. B. C. de Melo, Eur. Phys. J. C **79** (2019) no.2, 116
M. Peláez, U. Reinosa, J. Serreau, M. Tissier and N. Wschebor, Phys. Rev. D **96** (2017) no.11, 114011

QCD's greens functions from DSEs:

F. Gao, J. Papavassiliou and J. M. Pawlowski, Phys. Rev. D **103** (2021) no.9, 094013
A. C. Aguilar, M. N. Ferreira, J. Papavassiliou and L. R. Santos, Eur. Phys. J. C **84** (2024) no.7, 676
M. Q. Huber, Phys. Rev. D **101** (2020), 114009

and more...

Non-perturbative calculations for hadron phenomenology

Extensive work from many different groups to compute hadrc from non-perturbative analytical methods:

Z. N. Xu, Z. Q. Yao, D. Binosi, M. Ding, C. D. Roberts and J. Rodríguez-Quintero, Eur. Phys. J. C **85** (
G. Eichmann, A. Gómez, J. Horak, J. M. Pawlowski, J. Wessely and N. Wink, Phys. Rev. D **109** (2024)
M. Q. Huber, C. S. Fischer and H. Sanchis-Alepuz, Nuovo Cim. C **47** (2024) no.4, 184
G. Eichmann, E. Ferreira and A. Stadler, Phys. Rev. D **105** (2022) no.3, 034009

Lattice efforts to compute QCD's Green's functions:

M. Colaço, O. Oliveira and P. J. Silva, Phys. Rev. D **109** (2024) no.7, 074502
O. Oliveira, A. Kızılersu, P. J. Silva, J. I. Skullerud, A. Sternbeck and A. G. Williams, Acta Phys. Polon. Supp. **9** (2016), 363-368
O. Oliveira, W. de Paula, T. Frederico and J. P. B. C. de Melo, Eur. Phys. J. C **79** (2019) no.2, 116
M. Peláez, U. Reinosa, J. Serreau, M. Tissier and N. Wschebor, Phys. Rev. D **96** (2017) no.11, 114011

QCD's greens functions from DSEs:

F. Gao, J. Papavassiliou and J. M. Pawlowski, Phys. Rev. D **103** (2021) no.9, 094013
A. C. Aguilar, M. N. Ferreira, J. Papavassiliou and L. R. Santos, Eur. Phys. J. C **84** (2024) no.7, 676
M. Q. Huber, Phys. Rev. D **101** (2020), 114009

Outlook

1. Extending DSE solutions and lattice data to the complex plane
2. Meson decays and $^3P_0$ model from DSE data
3. Hybrid meson decays from DSE data

1. Extending DSE solutions and lattice data to the complex plane

Dyson-Schwinger equations

DSEs provide a powerful tool for recursively computing QCD's Green's Functions:

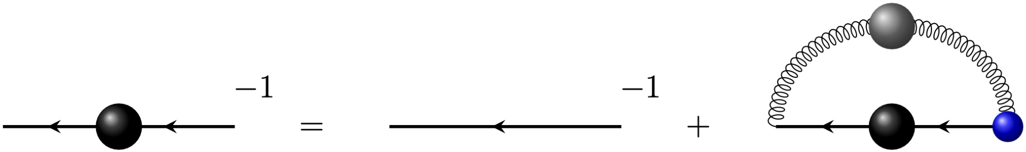

DSEs provide a powerful tool for recursively computing QCD's Green's Functions:

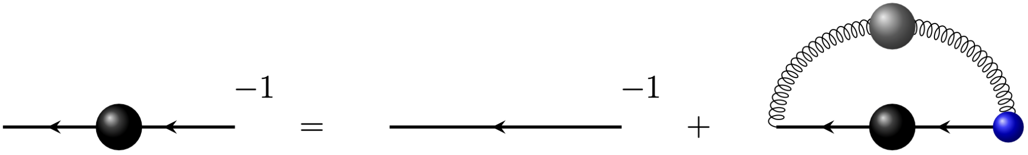

$$S(p) = \frac{Z_f(p)\,\not{p} + M(p)}{p^2 - M^2(p)}$$

Dyson-Schwinger equations

Truncations of DSEs can be chosen to mimic lattice behavior:

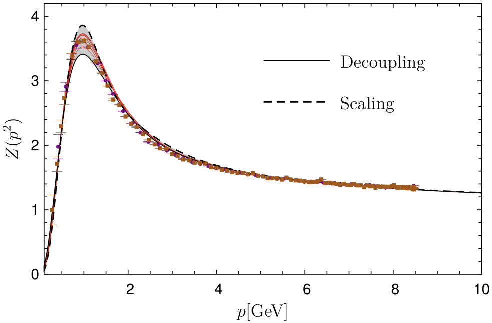

M. Q. Huber, Phys. Rev. D **101** (2020), 114009 doi:10.1103/PhysRevD.101.114009

Dyson-Schwinger equations

Simple parametrizations are also used to resemble lattice data:

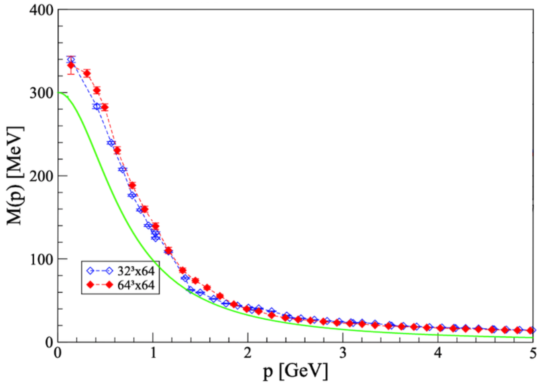

Data from: [O. Oliveira, A. Kızılersu, P. J. Silva, J. I. Skullerud, A. Sternbeck and A. G. Williams, Acta Phys. Polon. Supp. **9** (2016), 363-368]

Hence, DSEs provide data for Green's functions matching lattice data in the Euclidean side $p_E^2 > 0$.

How can we extend these results to the Minkowski regime $p_E^2 < 0$ in a reliable manner?

Hence, DSEs provide data for Green's functions matching lattice data in the Euclidean side $p_E^2 > 0$.

How can we extend these results to the Minkowski regime $p_E^2 < 0$ in a reliable manner?

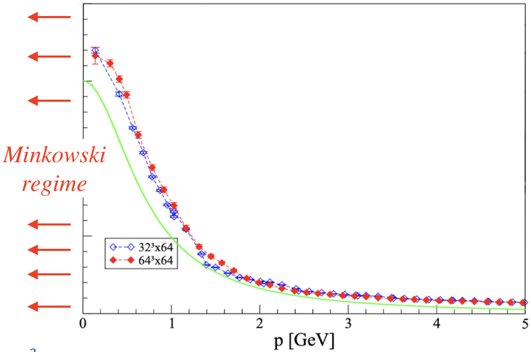

Venturing the complex plane

Several works study the analytic structure of QCD's Green's functions in the complex plane:

In QED: P. Maris, Phys. Rev. D **50** (1994), 4189-4193 doi:10.1103/PhysRevD.50.4189
QCD: P. Lowdon, Nucl. Phys. B **935** (2018), 242-255; O. Oliveira, T. Frederico and W. de Paula, Eur. Phys. J. C **85** (2025) no.3, 280

Venturing the complex plane

Several works study the analytic structure of QCD's Green's functions in the complex plane:
In QED: P. Maris, Phys. Rev. D **50** (1994), 4189-4193 doi:10.1103/PhysRevD.50.4189
QCD: P. Lowdon, Nucl. Phys. B **935** (2018), 242-255; O. Oliveira, T. Frederico and W. de Paula, Eur. Phys. J. C **85** (2025) no.3, 280

Anyhow, the analytic structure of correlation functions for confined particles remains unclear.

Venturing the complex plane

Several works study the analytic structure of QCD's Green's functions in the complex plane:
In QED: P. Maris, Phys. Rev. D **50** (1994), 4189-4193 doi:10.1103/PhysRevD.50.4189
QCD: P. Lowdon, Nucl. Phys. B **935** (2018), 242-255; O. Oliveira, T. Frederico and W. de Paula, Eur. Phys. J. C **85** (2025) no.3, 280

Anyhow, the analytic structure of correlation functions for confined particles remains unclear.

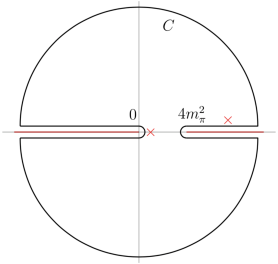

Dispersive approaches may suffer from systematic uncertainties.

Venturing the complex plane from lattice or DSE data

Given a finite set of lattice or DSE data $\{A_n\}$ at $p_E^2 = a_n$, we can construct infinitely many entire functions (we can even add poles and cuts) that match the data $F(a_n) = A_n$ for all n:

$$F(p_E^2) = \sum_{n=1}^{k} e^{\gamma_n (p_E^2 - a_n)} \frac{g(p_E^2)}{p_E^2 - a_n} \frac{A_n}{g'(a_n)}.$$

with the Weierstrass polynomial

$$g(p_E^2) = \prod_{n=1}^{k} \left(1 - \frac{p_E^2}{a_n}\right)$$

and arbitrary γ_n.

Infinitely many interpolator functions

Lattice or DSE

data $\{A_n\}$ at
$p_E^2 = a_n$

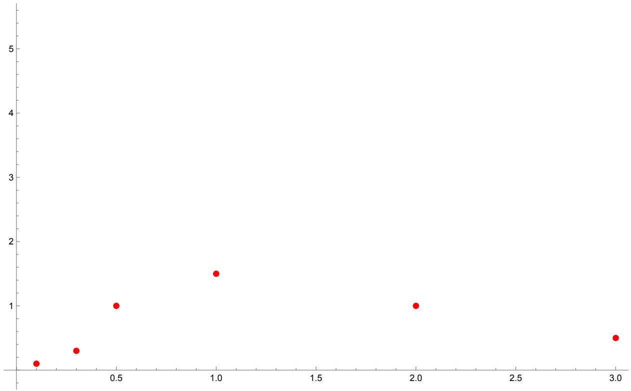

Infinitely many interpolator functions

Lattice or DSE data $\{A_n\}$ at $p_E^2 = a_n$

$$F(p_E^2) = \sum_{n=1}^{k} e^{\gamma_n (p_E^2 - a_n)} \frac{g(p_E^2)}{p_E^2 - a_n} \frac{A_n}{g'(a_n)}.$$

$\gamma_n = 0$ and

$\gamma_n = -3.1$

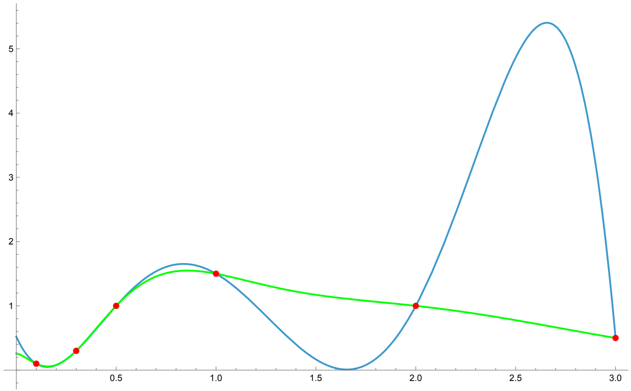

Lattice or DSE data $\{A_n\}$ at $p_E^2 = a_n$

$$F(p_E^2) = \sum_{n=1}^{k} \frac{g}{p_E^2}$$

Need assumptions!

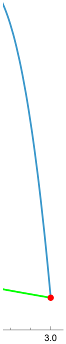

Venturing the complex plane: extracting a constituent quark mass

The first strategy is just extending the rational parametrizations to the Minkowski regime

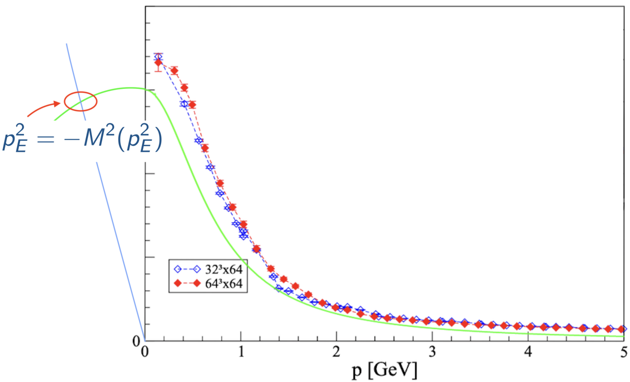

$$M(p^2) = M(0)\frac{\Lambda_B^2}{\Lambda_B^2 + p^2}$$

$$M(0) \simeq 0.32 \text{ GeV}, \ \Lambda_B \simeq 1 \text{ GeV}$$

Venturing the complex plane: extracting a constituent quark mass

Second, we can extend the Euclidean data analytically by numerically solving the Cauchy-Riemann equations for a function $f(z)$, $u = \mathrm{Re}(f(z))$, $v = \mathrm{Im}(f(z))$:

$$\frac{\partial v}{\partial y} = \frac{\partial u}{\partial x}$$
$$\frac{\partial u}{\partial y} = -\frac{\partial v}{\partial x} \ .$$

M. Gimeno-Segovia and F. J. Llanes-Estrada, Eur. Phys. J. C **56** (2008), 557-569

Change of complex variable $z \to \tilde{z} = \log(z)$. For $\tilde{z} = \tilde{x} + i\tilde{y}$ then $z = e^{\tilde{x}}(\cos\tilde{y}, \sin\tilde{y})$, to reach $z = (-|x|, 0)$ from $(|x|, 0)$. That is, we need to solve the CR equations on a rectangle in the $\tilde{z}$ plane, which in discretized form is

$$(\tilde{x}_i, 0) \to (\tilde{x}_i, \delta) \to (\tilde{x}_i, 2\delta) \cdots \to (\tilde{x}_i, n\delta = \pi) \ .$$

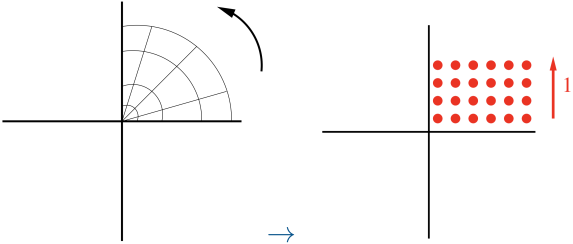

Venturing the complex plane: extracting a constituent quark mass

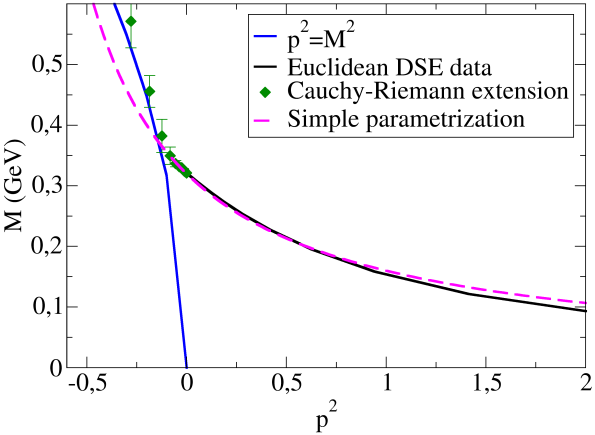

Venturing the complex plane: extracting a constituent quark mass

UNIVERSIDAD COMPLUTENSE MADRID

A third method is the famous Schlessinger point method. This method extends the data via a rational function by using the values of the function at different points (different from Padé approximants)

$$f(x) \simeq Sc(x) \equiv \cfrac{f_1}{1 + \cfrac{(x-x_1)a_1}{1 + \cfrac{(x-x_2)a_2}{1 + \cfrac{\cdots}{1 + (x - x_{N-1})a_{N-1}}}}}$$

R. A. Tripolt, I. Haritan, J. Wambach and N. Moiseyev, Phys. Lett. B **774** (2017), 411-416
D. Binosi, A. Pilloni and R. A. Tripolt, Phys. Lett. B **839** (2023), 137809 doi:10.1016/j.physletb.2023.137809

Venturing the complex plane: extracting a constituent quark mass

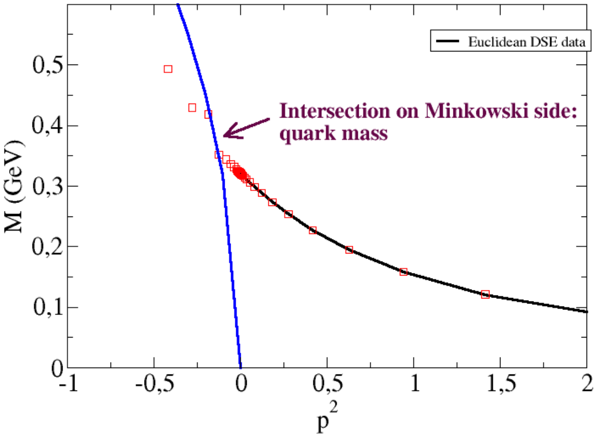

Venturing the complex plane: extracting a constituent quark mass

- Simple Parametrization:

  365(10) MeV

- Cauchy-Riemann equations:

  365(25) MeV

- Schlessinger:

  350(10) MeV

2. Meson decays and $^3P_0$ model from DSE data

Based on : Phys.Rev.D 109 (2024) 7, 074015

$q\bar{q}$ OZI-allowed meson decays

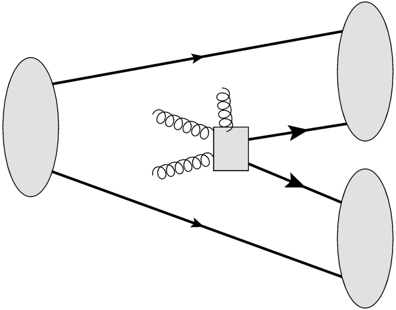

L. Micu, NPB 10 (1969) 521-526

$q\bar{q}$ OZI-allowed meson decays

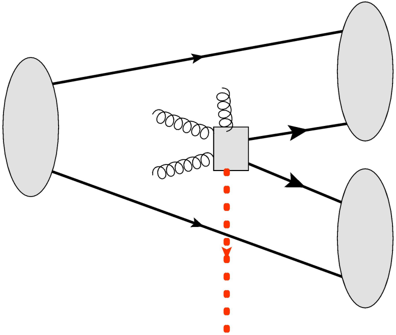

$${}^1S_0, {}^1P_1, {}^3S_1, {}^3P_0, {}^3P_1, {}^3P_2 \ldots {}^{2S+1}L_J$$

Possible Q# of produced pair

L. Micu, NPB 10 (1969) 521-526

$q\bar{q}$ OZI-allowed meson decays

A. Gómez-Nicola *et al.* PLB 606 351-360 (2005)

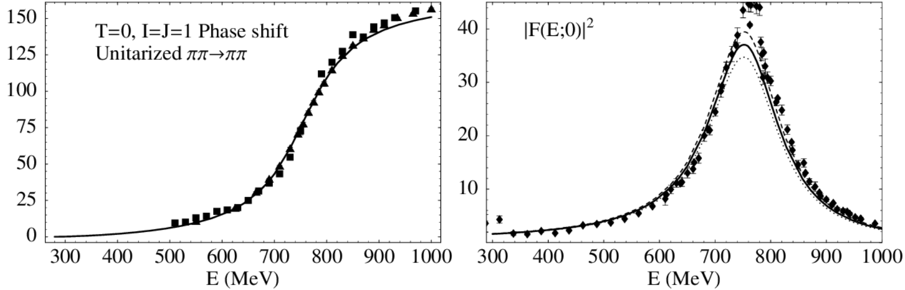

$$\cancel{^1S_0}, \cancel{^1P_1}, {}^3S_1, {}^3P_0, {}^3P_1, {}^3P_2 \ldots$$

Think of $\rho(\uparrow\uparrow) \to \pi(\uparrow\downarrow)\pi(\uparrow\downarrow)$

$q\bar{q}$ OZI-allowed meson decays

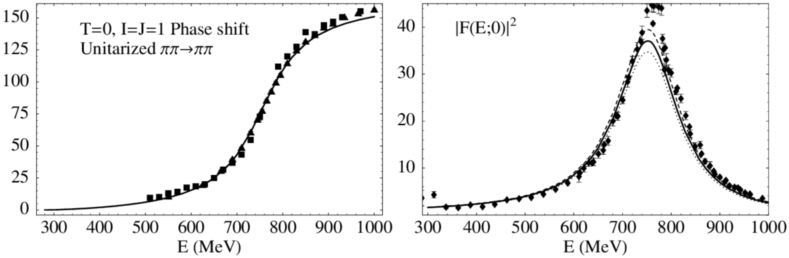

$$^1S_0, {}^1P_1, \cancel{^3S_1}, {}^3P_0, {}^3P_1, {}^3P_2 \ldots$$

Think of $\rho(\text{s-wave}) \to \underbrace{\pi(\text{s-wave})\pi(\text{s-wave})}_{L=1}$

Transition amplitude must carry a P wave.

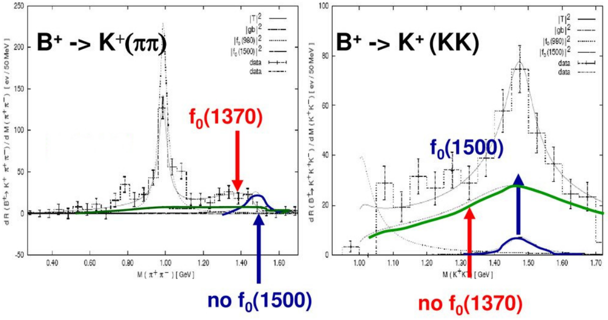

$$^1S_0, {}^1P_1, {}^3S_1, {}^3P_0, {}^3\not{P}_1, {}^3\not{P}_2 \ldots$$

Move on to $\underbrace{f_0}_{\text{mainly } ^3P_0} \to \underbrace{\pi\pi}_{J=0}$

E. Klempt `https://slideplayer.com/slide/14648261/`

Lore: important $^3P_0$ pair production mechanism

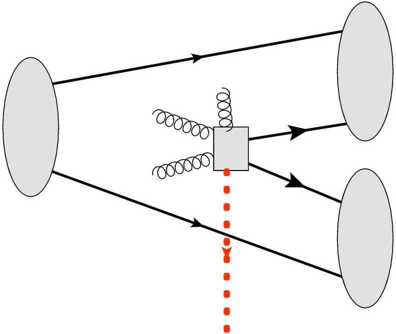

$$^1S_0, ^1P_1, ^3S_1, ^3P_0, ^3P_1, ^3P_2 \ldots ^{2S+1}L_J$$

Possible Q# of produced pair

L. Micu, NPB 10 (1969) 521-526

$^3P_0$ not visible in QCD (or QED)

- $\int d^3x \; \bar{\psi} \; \boldsymbol{\gamma} \cdot \boldsymbol{A} \; \psi$ seems $^3S_1$

$^3P_0$ not visible in QCD (or QED)

- $\int d^3x \; \bar{\psi} \; \gamma \cdot \boldsymbol{A} \; \psi$ seems $^3S_1$
- Chiral-symmetry respecting at all orders in perturbation theory

$^3P_0$ not visible in QCD (or QED)

UNIVERSIDAD COMPLUTENSE MADRID

- $\int d^3x\ \bar{\psi}\ \boldsymbol{\gamma}\cdot\boldsymbol{A}\ \psi$ seems $^3S_1$
- Chiral-symmetry respecting at all orders in perturbation theory
- But $^3P_0$ breaks chiral symmetry

Modelling the D/D_s spectrum with $^3P_0$: 32 modes studied by Close and Swanson

F. Close and E.S.Swanson PRD**72** 094004 (2005)

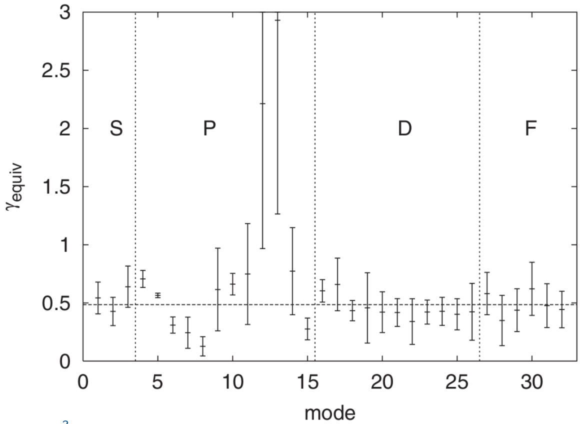

$^3P_0$ Effective Hamiltonian

$$H_{^3P_0} = \sqrt{3} g_s \int d^3\boldsymbol{x} \bar{\psi}(\boldsymbol{x}) \psi(\boldsymbol{x})$$

$\gamma = \frac{g_s}{2m}$

$^3P_0$ Effective Hamiltonian

$$H_{^3P_0} = \sqrt{3} g_s \int d^3\boldsymbol{x} \bar{\psi}(\boldsymbol{x}) \psi(\boldsymbol{x})$$

$\gamma = \frac{g_s}{2m}$ Chiral-symmetry breaking:

$$[Q_5, H_{^3P_0}] = \left[\int d^3\boldsymbol{x} \psi^\dagger(\boldsymbol{x}) \gamma_5 \psi(\boldsymbol{x}), H_{^3P_0} \right] \neq 0$$

$^3P_0$ Effective Hamiltonian

UNIVERSIDAD COMPLUTENSE MADRID

$$H_{^3P_0} = \sqrt{3}g_s \int d^3\boldsymbol{x}\bar{\psi}(\boldsymbol{x})\psi(\boldsymbol{x})$$

$\gamma = \frac{g_s}{2m}$ Chiral-symmetry breaking:

$$[Q_5, H_{^3P_0}] = \left[\int d^3\boldsymbol{x}\psi^\dagger(\boldsymbol{x})\gamma_5\psi(\boldsymbol{x}), H_{^3P_0}\right] \neq 0$$

$$i(2\pi)^4\delta^{(4)}(p+q)\mathcal{M}^{ss'}_{^3P_0}(p,q) = \langle \boldsymbol{p}s, \boldsymbol{q}s'|iT_{^3P_0}|0\rangle =$$
$$= (i\,(2\pi)^4\delta^{(4)}(p+q))(-\sqrt{3}g_s)\bar{u}^s(p)v^{s'}(q)$$

$$\boxed{\Rightarrow \bar{u}^s(\boldsymbol{p})v^{s'}(-\boldsymbol{p}) = 2\boldsymbol{p}\cdot\boldsymbol{\sigma}^{ss'}}$$

$^3P_0$ coupling dependence on the quark mass by Salamanca group

J. Segovia, D. R. Entem, F. Fernández Phys.Lett.B **715** (2012) 322-327

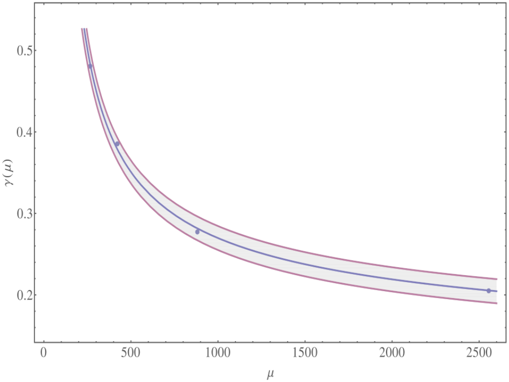

$^3P_0$ coupling dependence on the quark mass by Salamanca group

J. Segovia, D. R. Entem, F. Fernández Phys.Lett.B **715** (2012) 322-327

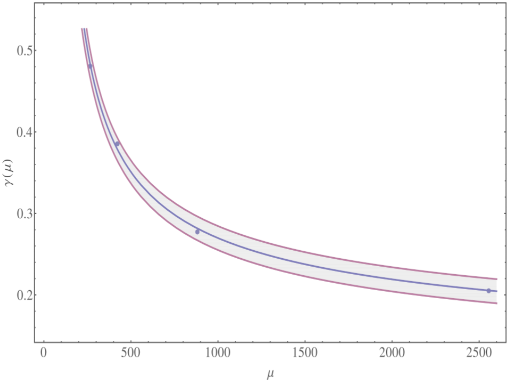

Recent work pointing towards the direction that this sub-process may also have a measurable impact on hadron structure: 2406.05920 M. Karliner and J.L. Rosner.

Our work:
connect Quark-model pheno w. Landau gauge QCD

Can we obtain the $^3P_0$ effective Hamiltonian from *ab initio* QCD calculations?

Our work:
connect Quark-model pheno w. Landau gauge QCD

UNIVERSIDAD COMPLUTENSE MADRID

Can we obtain the $^3P_0$ effective Hamiltonian from *ab initio* QCD calculations?

- N-gluon to $\bar{q}q$ kernel not known from first principles
- What to do with the information at hand?

Strategy: couple dynamical quarks to the flux tube background

Flux tube $\longleftrightarrow$ Dynamical quarks

Strategy: couple dynamical quarks to the flux tube background

Flux tube $\longleftrightarrow$ Dynamical quarks

Through Landau-gauge DSE primitive QCD Green's functions

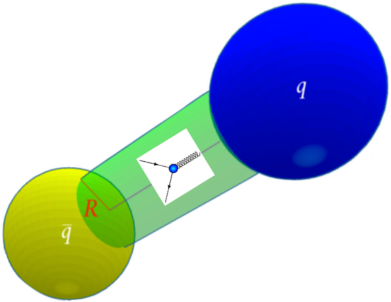

Quark-Gluon vertex spin structure

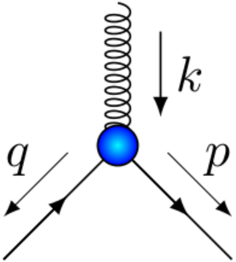

$$\Gamma^{\mu}_{T}(q_E, p_E; k_E) = \sum_{i=1}^{8} g_i(\bar{p}_E^2)\rho_i^{\mu}(q_E, p_E)$$

$$k^{\mu} = p^{\mu} + q^{\mu}$$

- It includes chiral-symmetry respecting and breaking pieces

Parametrization of transverse part of the vertex

- The tree-level vertex $\rho^{\mu}_{1,E} = (\delta^{\mu\nu} - \hat{k}^{\mu}_{E}\hat{k}^{\nu}_{E})\gamma^{\mu}_{E} \equiv \gamma^{\mu}_{T,E}$

  with $\quad g_1(x) = 1 + \frac{1.67+0.204x}{1+0.683x+0.000851x^2}$

Parametrization of transverse part of the vertex

- Chiral-symmetry breaking structures $(s_E^\mu = (\delta^{\mu\nu} - \hat{k}_E^\mu \hat{k}_E^\nu)\bar{p}_E^\nu)$

$$\rho^\mu_{2,E} = i\hat{s}^\mu_E \quad \text{and} \quad \rho^\mu_{3,E} = i\hat{\not{k}}_E \gamma^\mu_{T,E}$$

$$\text{with} \quad g_3(x) = -1.45 g_2(x) = \frac{0.365x}{0.0187 + 0.353x + x^2} \; ;$$

Parametrization of Landau-transverse part of the vertex

- The chirally symmetric structures

$$\rho^{\mu}_{4,E} = \hat{\not{k}}_E s^{\mu}_E \quad \text{and} \quad \rho^{\mu}_{7,E} = \hat{\not{s}}_E \hat{\not{k}}_E \gamma^{\mu}_{T,E}$$

$$\text{with} \quad g_4(x) = g_7(x) = \frac{2.59x}{0.859+3.27x+x^2} \, .$$

Euclidean q_E^2 functions (input from lattice, DSEs)

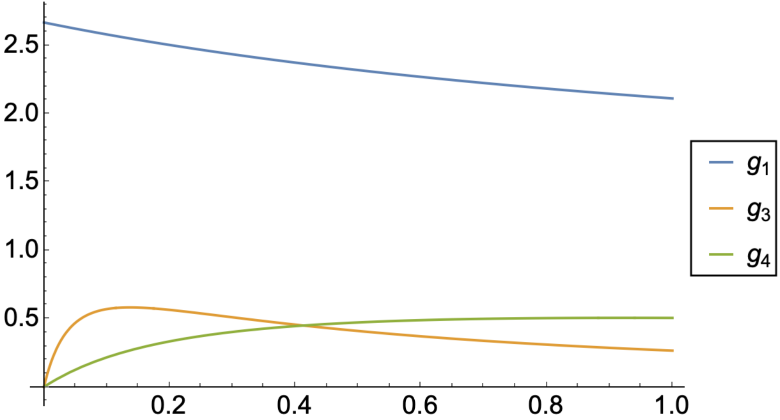

Naive extension to physical Minkowski space

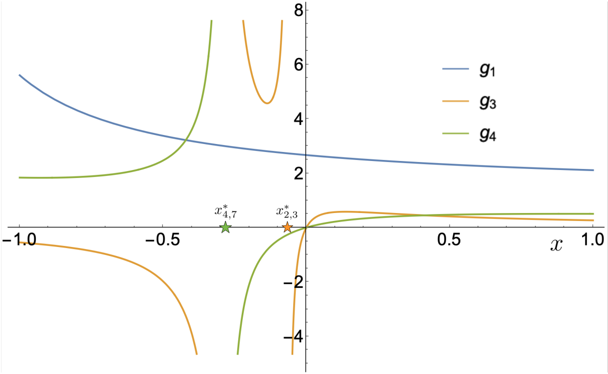

Note the $Q^2 < 0$ enhancement of the chiral symmetry breaking piece!

To get a color singlet:

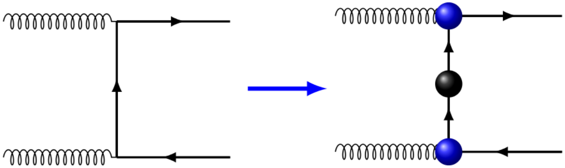

Breit-Wheeler process for $q\bar{q}$ creation

To get a color singlet:

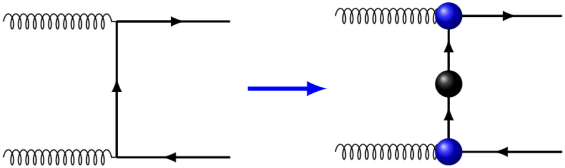

We couple flux-tube "gluons" to the quarks with the DSE functions

In a constant chromoelectric flux tube:

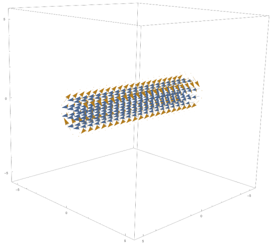

- Simplify to a constant chromo-E (parallel-plate capacitor) Background Landau-gauge field $(A_\rho, A_\theta, A_z, A_0) = (0, 0, 0, -Ez)$

In a constant chromoelectric flux tube:

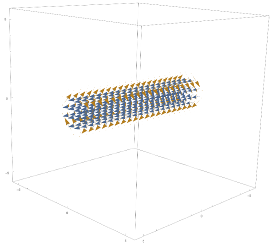

- Simplify to a constant chromo-E (parallel-plate capacitor) Background Landau-gauge field $(A_\rho, A_\theta, A_z, A_0) = (0, 0, 0, -Ez)$
- Think of the Schwinger pair-creation mechanism in QED.

In a constant chromoelectric flux tube:

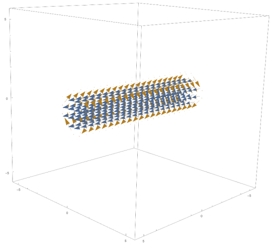

- Simplify to a constant chromo-E (parallel-plate capacitor) Background Landau-gauge field $(A_\rho, A_\theta, A_z, A_0) = (0, 0, 0, -Ez)$
- Think of the Schwinger pair-creation mechanism in QED.
- Rotation symmetry is broken: **must use notation for diatomic molecules!**. ${}^3P_0 \to {}^3\Pi_0$.

$$\langle \boldsymbol{p}s, \boldsymbol{q}s'|iT_{\text{singlet}}|0\rangle =$$

$$\langle \boldsymbol{p}s, \boldsymbol{q}s'| - \frac{g^2}{2}\int d^4x\bar{\psi}_i(x)T^a_{ij}A^a_\mu(x)\Gamma^\mu\psi_j(x)\int d^4y\bar{\psi}_i(y)T^a_{ij}A^a_\nu(y)\Gamma^\nu\psi_j(y)|0\rangle =$$

$$= -g^2\int d^4xd^4y\int\frac{d^4t}{(2\pi)^4}\tilde{A}^a_0(p-t)\tilde{A}^a_0(q+t)\mathcal{K}^{ss'}_{ab}(p,q,t)$$

where

$$\mathcal{K}^{ss'}_{ab}(p,q,t) \equiv \left[\bar{u}^s_i(p)T^a_{ij}\Gamma^0(p,-t)S(t)T^b_{jk}\Gamma^0(q,t)v^{s'}_k(q)\right]$$

and $S(t)$ is the dressed fermion propagator.

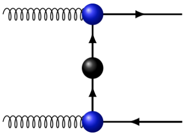

A relation between the gluon to quark kernel $\mathcal{K}$ and the pair production amplitude

UNIVERSIDAD COMPLUTENSE MADRID

For the constant chromoelectric background $\tilde{A}_0^a(p) \propto \partial/\partial p^3$:

$$\langle \boldsymbol{p}s, \boldsymbol{q}s'|iT_{\text{singlet}}|0\rangle = -(2\pi)^4\delta^{(4)}(p+q)(gE)^2 \left[\frac{\partial}{\partial p^3}\frac{\partial}{\partial q^3}\mathcal{K}_{ab}^{ss'}(p,q,t)\right]\Big|_{t=-q}$$

- With the primitive Green's functions construct this skeleton kernel ✓
- Project it over ${}^{2S+1}L_J$ and numerically compare
  (But you can see that the chiral symmetry breaking part will be important, perhaps even dominant)

Angular Momentum projections

$$\mathcal{A}^{{}^1S_0}(|\boldsymbol{p}|) = \sum_s \int d\Omega\, \mathcal{A}^{ss}(\boldsymbol{p}) \qquad \mathcal{A}_i^{{}^3S_1}(|\boldsymbol{p}|) = \sum_{s,t} \int d\Omega\, \boldsymbol{\sigma}_i^{st} \mathcal{A}^{ts}(\boldsymbol{p})$$

$$\mathcal{A}^{{}^3P_0}(|\boldsymbol{p}|) = \sum_{s,t} \int d\Omega\, \hat{\boldsymbol{p}} \cdot \boldsymbol{\sigma}^{st} \mathcal{A}^{ts}(\boldsymbol{p}) \qquad \mathcal{A}_i^{{}^1P_1}(|\boldsymbol{p}|) = \sum_s \int d\Omega\, \hat{\boldsymbol{p}}_i\, \mathcal{A}^{ss}(\boldsymbol{p})\,.$$

Remember spherical symmetry is reduced to cylindrical symmetry:

$$\mathcal{A} = A\sigma_\perp \cdot \mathbf{p}_\perp + B\sigma_z p_z + C\sigma_\perp + D\sigma_z$$

Angular Momentum projections

$$\mathcal{A}^{{}^1S_0}(|\boldsymbol{p}|) = \sum_s \int d\Omega\, \mathcal{A}^{ss}(\boldsymbol{p}) \qquad \mathcal{A}_i^{{}^3S_1}(|\boldsymbol{p}|) = \sum_{s,t} \int d\Omega\, \boldsymbol{\sigma}_i^{st} \mathcal{A}^{ts}(\boldsymbol{p})$$

$$\mathcal{A}^{{}^3P_0}(|\boldsymbol{p}|) = \sum_{s,t} \int d\Omega\, \hat{\boldsymbol{p}} \cdot \boldsymbol{\sigma}^{st} \mathcal{A}^{ts}(\boldsymbol{p}) \qquad \mathcal{A}_i^{{}^1P_1}(|\boldsymbol{p}|) = \sum_s \int d\Omega\, \hat{\boldsymbol{p}}_i\, \mathcal{A}^{ss}(\boldsymbol{p})\,.$$

Remember spherical symmetry is reduced to cylindrical symmetry:

$$\mathcal{A} = A\sigma_\perp \cdot \mathbf{p}_\perp + B\sigma_z p_z + C\sigma_\perp + D\sigma_z$$

Use ${}^{2S+1}\Lambda_{j_z}$ quantum numbers.

QED computation

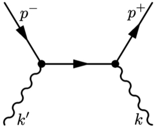

For a $(A_\rho, A_\theta, A_z, A_0) = (0,0,0,-Ez)$

$$\frac{\partial}{\partial p_-^3}\frac{\partial}{\partial p_+^3}\left[\bar{u}^s(\boldsymbol{p}_+)\left(\gamma^0 - \frac{(\not{p}_+ - \not{t})}{p_+^0}\right)\frac{\not{t}+m}{t^2-m^2}\left(\gamma^0 - \frac{(\not{p}_- + \not{t})}{p_-^0}\right)v^{s'}(\boldsymbol{p}_-)\right]\Big|_{\boldsymbol{t}=-\boldsymbol{q}=\boldsymbol{p}}.$$

QED computation

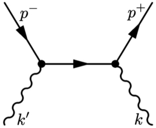

For a $(A_\rho, A_\theta, A_z, A_0) = (0, 0, 0, -Ez)$

$$\frac{\partial}{\partial p_-^3}\frac{\partial}{\partial p_+^3}\left[\bar{u}^s(\boldsymbol{p}_+)\left(\gamma^0 - \frac{(\not{p}_+ - \not{t})}{p_+^0}\right)\frac{\not{t}+m}{t^2-m^2}\left(\gamma^0 - \frac{(\not{p}_- + \not{t})}{p_-^0}\right)v^{s'}(\boldsymbol{p}_-)\right]\Bigg|_{\boldsymbol{t}=-\boldsymbol{q}=\boldsymbol{p}} .$$

This has a $^3P_0$ contribution:

$$\mathcal{A}^{^3\Sigma_1}_{\text{QED}}(|\boldsymbol{p}|) \propto -2\pi|\boldsymbol{p}|\left(\frac{E_{\boldsymbol{p}}-m}{E_{\boldsymbol{p}}^4}\right) \quad \mathcal{A}^{^3\Pi_0}_{\text{QED}}(|\boldsymbol{p}|) \propto \frac{32m|\boldsymbol{p}|}{3E_{\boldsymbol{p}}^4} . \quad \Rightarrow \frac{\mathcal{A}^{^3\Pi_0}_{\text{QED}}}{\mathcal{A}^{^3\Sigma_1}_{\text{QED}}} = O\left(\frac{m^2}{|\mathbf{p}|^2}\right)$$

QED comparison of two field insertions

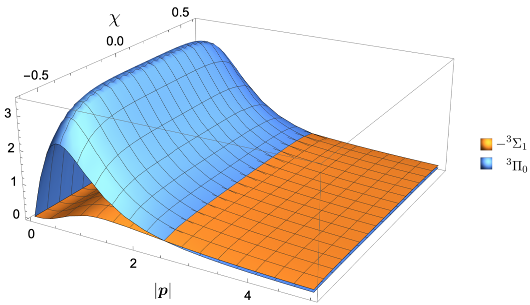

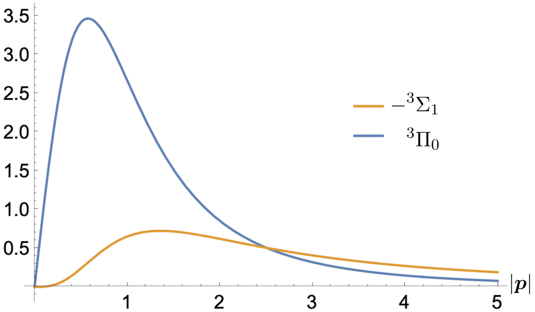

In QCD: two field insertions for getting the singlet

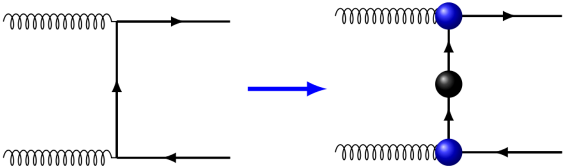

Skeleton-expanded kernel.

In QCD: two field insertions for getting the singlet

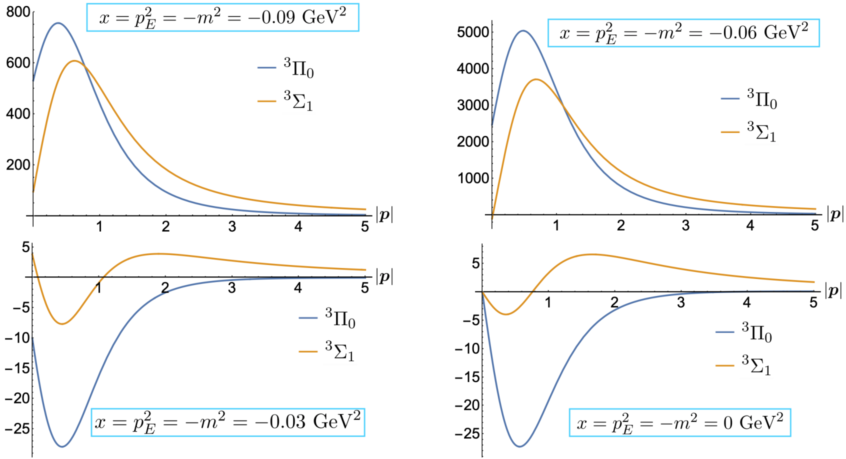

In QCD: two field insertions for getting the singlet

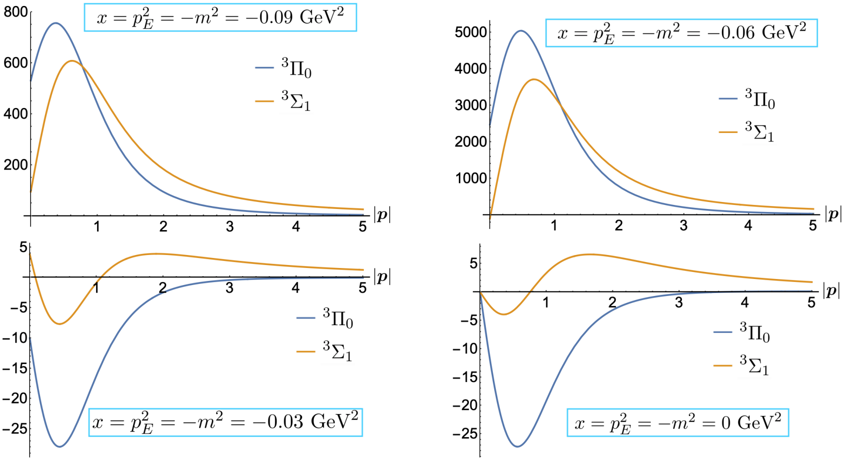

Grounding the ${}^3P_0$ with Landau Gauge DSE data

${}^3\Sigma_1$ dominates at high momenta: spontaneous chiral symmetry breaking is less important.

Grounding the $^3P_0$ with Landau Gauge DSE data

$^3\Sigma_1$ dominates at high momenta: spontaneous chiral symmetry breaking is less important.
$^3P_0$ dominates at low momenta! At threshold:

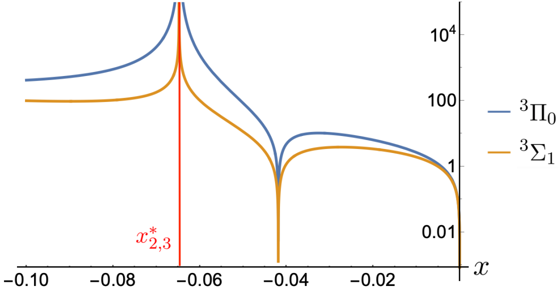

Grounding the $^3P_0$ with Landau Gauge DSE data

$^3\Sigma_1$ dominates at high momenta: spontaneous chiral symmetry breaking is less important.
$^3P_0$ dominates at low momenta! At threshold:

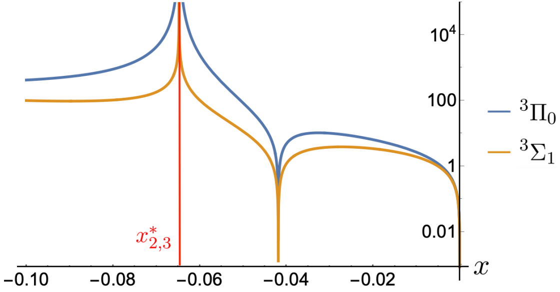

Recent work suggests the failure of $^3P_0$ at high $q\bar{q}$ relative momenta:
R. Bruschini, P. González and T. Tarutina, Phys. Rev. D **111** (2025) no.7, 074042 doi:10.1103/PhysRevD.111.074042

$^3P_0$ vs. $^3\Pi_0$

$^3\Pi_0$ requires $m_L = 1 \implies L \geq 1$, without restricting total J, the smallest angular momenta is $^3P_0$. To distinguish $^3P_0$ and $^3\Pi_0$ does not seem possible with basic meson decays, interpreted as $(q\bar{q}) \to (q\bar{q})(q\bar{q})$.

${}^3P_0$ vs. ${}^3\Pi_0$

${}^3\Pi_0$ requires $m_L = 1 \implies L \geq 1$, without restricting total J, the smallest angular momenta is ${}^3P_0$. To distinguish ${}^3P_0$ and ${}^3\Pi_0$ does not seem possible with basic meson decays, interpreted as $(q\bar{q}) \to (q\bar{q})(q\bar{q})$.

For the parent meson, spin is $s_i = 0, 1$, internal orbital angular momentum l, and parity $P_i = (-1)^{l+1}$. The two daughter mesons in the final state have $s_f = 0, 1, 2$, internal and relative orbital l_1, l_2, L and parity (one antiparticle has been produced) $P_f = (-1)^{l_1+l_2+L+2}$, $\Rightarrow$ orbital angular momentum has to change by an odd number of units to preserve parity.

${}^3P_0$ vs. ${}^3\Pi_0$

UNIVERSIDAD COMPLUTENSE MADRID

${}^3\Pi_0$ requires $m_L = 1 \implies L \geq 1$, without restricting total J, the smallest angular momenta is ${}^3P_0$. To distinguish ${}^3P_0$ and ${}^3\Pi_0$ does not seem possible with basic meson decays, interpreted as $(q\bar{q}) \to (q\bar{q})(q\bar{q})$.

For the parent meson, spin is $s_i = 0, 1$, internal orbital angular momentum l, and parity $P_i = (-1)^{l+1}$. The two daughter mesons in the final state have $s_f = 0, 1, 2$, internal and relative orbital l_1, l_2, L and parity (one antiparticle has been produced) $P_f = (-1)^{l_1+l_2+L+2}$, $\Rightarrow$ orbital angular momentum has to change by an odd number of units to preserve parity.

Total angular momentum conservation implies that $\Delta J = 0$, $\Rightarrow |\Delta S| = |\Delta L|$.
Because $\Delta S = 0, \pm(1, 2)$, these are the values that ΔL can take. Among them, $\Delta L = 1$ is common to both ${}^3P_0$ and ${}^3\Pi_0$, $\Delta L = 0$ to none, and only $\Delta L = 2$ could distinguish the two mechanisms.
Not allowed by parity conservation!

Recap

- Historical $^3P_0$ mechanism of strong decays needs QCD grounding.

Recap

- Historical $^3P_0$ mechanism of strong decays needs QCD grounding.
- A first scan, clearly shows $^3\Pi_0$ dominance at lower momenta. Supporting quark-model lore for $^3P_0$ quark-antiquark pair creation for meson decays.

Recap

- Historical $^3P_0$ mechanism of strong decays needs QCD grounding.
- A first scan, clearly shows $^3\Pi_0$ dominance at lower momenta. Supporting quark-model lore for $^3P_0$ quark-antiquark pair creation for meson decays.
- Distinguishing $^3P_0$ from $^3\Pi_0$ may not be straightforward.

Recap

- Historical ${}^3P_0$ mechanism of strong decays needs QCD grounding.
- A first scan, clearly shows ${}^3\Pi_0$ dominance at lower momenta. Supporting quark-model lore for ${}^3P_0$ quark-antiquark pair creation for meson decays.
- Distinguishing ${}^3P_0$ from ${}^3\Pi_0$ may not be straightforward.
- To do: use Cauchy-Riemann and Schlessinger extensions for the qqg vertex. More formal approaches: complete effective action treatment of the decay.

3. Hybrid meson decays from DSE data

Mounting evidence for exotic states

At present, there is strong indications of the existence of exotic hadrons ($qq\bar{q}\bar{q}$, $q\bar{q}g$,...)
Multiquark candidates:

- Tetraquarks ($cs\bar{u}\bar{d}$—LHCb 2020; $cu\bar{d}\bar{s}$, $cd\bar{u}\bar{s}$—LHCb 2022; $cc\bar{u}\bar{d}$—LHCb 2021; $cu\bar{c}\bar{s}$—LHCb 2021; $cd\bar{c}\bar{s}$—LHCb 2023; $cs\bar{c}\bar{s}$—CMS 2013, LHCb 2016, 2021, 2022; $cccc$—LHCb 2020, ATLAS 2023, CMS 2024)
- Pentaquarks ($qqqq\bar{q}$) ($uudc\bar{c}$—LHCb 2015, 2019; $udsc\bar{c}$—LHCb 2022).

Mounting evidence for exotic states

Some candidates that could be hybrid $q\bar{q}g$ mesons:

- The exotic candidate $\pi(1800)$ ($J^{PC} = 0^{-+}$).
- In $J/\psi \to \gamma\eta\eta'$ there is observation of the so called $\eta_1(1855)$ ($J^{PC} = 1^{-+}$).
- ...

Identifying a hybrid meson via signatures in its decay modes

For example: the candidate $\pi(1800)$ decays preferably into $S+P$ modes like $f_0\pi$ and $K_0^*\bar{K}$ whereas ordinary meson decay modes may be different:

$\Rightarrow$ useful to compare decay modes of canonical and hybrid mesons.

$^3P_0$ and Coulomb decay models disallow the decay of the excited pion $\pi(3S, 1850)$ to $b_1\pi$ whereas this is allowed for the hybrid meson $\pi(1800)$ $\Rightarrow$ **Smoking gun process**

C. Farina and E. S. Swanson, "Constituent model of light hybrid meson decays," Phys. Rev. D **109** (2024) no.9, 094015 doi:10.1103/PhysRevD.109.094015

Ongoing work in collaboration with R. Alkofer, G. Wieland and E. Swanson

A relatively "low hanging fruit" is studying the decays of hybrid mesons with DSE's functions:

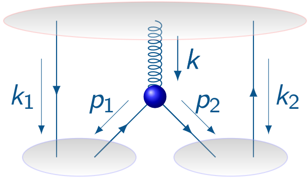

Instead of the simple ${}^3P_0$ model.

Ongoing work in collaboration with R. Alkofer, G. Wieland and E. Swanson

We may obtain angular momentum selection rules from projecting the "dressed" qqg kernel:

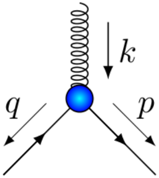

$$\langle \boldsymbol{p}_1 s, \boldsymbol{p}_2 s' | i T^a_{\text{octet}} | \mathbf{k} \lambda \rangle =$$

$$= \langle \boldsymbol{p}_1 s, \boldsymbol{p}_2 s' | - ig \int d^4 x \bar{\psi}_i(x) T^a_{ij} A^a_\mu(x) \Gamma^\mu(x) \psi_j(x) | \mathbf{k} \lambda \rangle =$$

$$= -ig \delta^{(4)}(p_1 + p_2 - k) T^a_{ij} t^\mu_{ij\ ss'\lambda}(\mathbf{k}, \mathbf{q}) \ ,$$

by projecting into spherical harmonics

$$t^\mu_{ij\ ss'\lambda}(\boldsymbol{k}, \boldsymbol{q}) = \sum_{l_g, l_q, m_g, m_q} Y^{m_g}_{l_g}(\hat{\mathbf{k}}) Y^{m_q}_{l_q}(\hat{\mathbf{q}}) \mathcal{Y}^{l_g, l_q m_g, m_q}_{ij\ ss'\lambda}(|\boldsymbol{k}|, |\mathbf{q}|)$$

Use this transition amplitude for the decay of the hybrid

We need hence to compute the amplitude for the decay $A \to B + C$ as $\langle B, C| \, iT_{\rm octet} \, |A\rangle$ to obtain the selection rules.

We need some input for the constituent gluon and the meson wavefunctions.

Use this transition amplitude for the decay of the hybrid

We need hence to compute the amplitude for the decay $A \to B + C$ as $\langle B, C|\, iT_{\rm octet}\, |A\rangle$ to obtain the selection rules.

We need some input for the constituent gluon and the meson wavefunctions.

Stay tuned!

Thank you!

MINISTERIO DE CIENCIA E INNOVACIÓN

UNIÓN EUROPEA
FONDO EUROPEO DE DESARROLLO REGIONAL
"Una manera de hacer Europa"

AGENCIA ESTATAL DE INVESTIGACIÓN

Funded by research grant PID2022-137003NB-I00 from spanish MCIN/AEI/10.13039/501100011033/ and EU FEDER